ELSEVIER

Analytica Chimica Acta 385 (1999) 257–264

ANALYTICA CHIMICA ACTA

Microelectrode arrays: application in batch-injection analysis

Denise A. Fungaro[a,b], Christopher M.A. Brett[a,*]

[a]*Departamento de Química, Universidade de Coimbra, P-3049 Coimbra, Portugal*
[b]*Instituto de Pesquisas Energéticas e Nucleares, Divisão de Química Ambiental, Universidade de São Paulo, Travessa R, 400, CEP 05508-900, São Paulo, SP, Brazil*

Received 14 July 1998; received in revised form 2 October 1998; accepted 4 October 1998

Abstract

The application of microelectrode arrays in electrochemical batch-injection analysis, injection volumes≤100 μl, has been investigated using a random array of microdisks (RAM) electrode made with carbon fibres. Preliminary batch-injection experiments involving hexacyanoferrate(II) oxidation, using fixed-potential amperometry and cyclic voltammetry, showed the expected lesser dependence on injection flow rate and the steady-state current characteristics of the RAM electrode, compared to results from similar experiments at macroelectrodes. After electrodepositing mercury on the carbon fibre disks, square wave anodic stripping voltammetry of the test of heavy metals zinc, cadmium and lead was carried out by batch-injection analysis. It was found that the accumulation time of the metals influenced the response to a greater extent than at macroelectrodes, that the influence on the injected volume was similar to that at macroelectrodes and the influence of injection flow rate was less. Detection limits are improved at the RAM electrode; sensitivity as a function of normalised electrode area is also enhanced. Experiments in which the RAM electrode was covered by a thin Nafion film before carrying out BIA–SWASV were also performed, and showed similar trends. Although BIA can be performed directly on real samples without added electrolyte, the combination with microelectrodes, which by themselves permit measurements in highly resistive media and fast scan rates, may prove to be very valuable in extreme situations.

Keywords: Microelectrodes; Microelectrode arrays; RAM electrodes; Batch-injection analysis; Trace metals; Anodic stripping voltammetry

1. Introduction

The advantages which can arise from the use of microelectrodes have been extensively documented, e.g. [1–3]. These include enhanced current densities, due to the hemispherical diffusion field which they induce, a lack of sensitivity to solution flow, and the ability to be used in highly resistive media, since the ohmic drop is small.

One way of exploiting the advantages of microelectrodes whilst ensuring large total currents is to use microelectrode arrays, in which each microelectrode has the same function. If these microelectrodes are sufficiently far apart from each other then the array acts as the sum of the individual responses. If they are very close then the array behaves as a macroelectrode with dimensions equal to that of the assembly [4]. Signal-to-noise ratios are improved by using microelectrode arrays, since the noise levels depend on the active area of the electrodes whereas the signal depends on the total area of the diffusion field [5].

*Corresponding author. Fax: +351-39-835295; e-mail: brett@cygnus.ci.uc.pt

0003-2670/99/$ – see front matter
PII: S0003-2670(98)00699-0

Comparisons between macroelectrodes and microelectrode arrays have been undertaken [6].

In the electrochemical batch-injection analysis (BIA) technique [7,8] an aliquot of sample of less than 100 μl is injected from a micropipette directly over the centre of an electrode immersed in electrolyte solution in an electrochemical cell. Apart from fixed-potential amperometric detection [8], applications to voltammetry [9], anodic stripping voltammetry [10,11] and adsorptive stripping voltammetry [12] have been described.

The purpose of this work is to see what advantages can arise from the use of microelectrode arrays instead of a macroelectrode in electrochemical BIA, particularly in terms of sensitivity to flow rate and current intensity enhancement, and with application to anodic stripping voltammetry at mercury microelectrode arrays.

2. Experimental

The batch-injection cell has been described previously [8]. Briefly, it consists of a modified large-volume wall-jet cell made of Perspex, filled with inert electrolyte, in which the inlet is replaced by the tip of a micropipette, internal diameter 0.47 mm, placed perpendicularly at a distance of 2–3 mm above the working electrode. The cell contains a Pt auxiliary electrode and a saturated calomel electrode (SCE) as reference. In this study the working electrode which is screwed in from the bottom of the cell was a RAM (Random Array of Microdisks) electrode (CSIRO, Melbourne, Australia), a gift from Dr. S. Fletcher, CSIRO. This nominally consisted of approximately 3200 carbon fibres of diameter~7.0 μm embedded in resin, 20–40% of which are active [13] – as supplied the number of active disks was specified as 667. These are enclosed within a total area of 0.28 cm^2, corresponding to a diameter of 0.6 cm. Before use, the RAM electrode was polished using diamond spray down to 1 μm particle size.

Injections were done from a Rainin EDP-Plus 100 programmable, motorised, electronic micropipette at calibrated flow rates of 24.5, 47.6 or 75.3 μl s^{-1}. Solutions were made from analytical grade reagents and Millipore Milli-Q water (resistivity≥18 MΩ cm).

Experiments were conducted using a BAS CV-50W potentiostat (Bioanalytical Systems, W. Lafayette, Indian, USA) controlled by Model 2.0 software.

Preparation of mercury microelectrode arrays was done in situ in the BIA cell by injection of 100 μl of 0.10 M Hg^{2+} contained in background electrolyte 0.10 M KNO_3+5 mM HNO_3. The applied potential was −1.0 V vs. SCE for 30 s. For comparative studies, mercury thin-film electrodes (MTFE) were made on a glassy carbon disk substrate (d=0.5 cm) by exactly the same procedure.

Nafion coatings on the RAM electrode were made in a similar way to the procedure described in [11] by applying 5 μl of 0.25% (w/v) Nafion solution to the electrode surface with the micropipette, followed immediately by 3 μl of *N*,*N*′-dimethylformamide casting solvent. The solvents were evaporated in a warm air stream from an air gun while the electrode was rotated at 50 rpm for 30 s. The polymer was then cured for 60 s in a hot air stream (~70°C). Using the density of bulk Nafion [14] the thickness of the Nafion film was estimated to be of the order of 1 μm. The coated electrode was placed in the BIA cell and mercury deposition was done in situ by injecting 10 μl of a solution of 0.10 M Hg^{2+} in 0.10 M KNO_3+5 mM HNO_3. The applied potential was −1.0 V vs. SCE for 64 s.

3. Results and discussion

The main objective of this study is to evaluate the advantages of the utilisation of RAM electrodes in batch-injection analysis–anodic stripping voltammetry (BIA–ASV). However, initial experiments are designed to evaluate the differences in fixed-potential amperometry and cyclic voltammetry compared to macroelectrodes using the oxidation of hexacyanoferrate(II) in 0.4 M K_2SO_4 electrolyte as test system.

3.1. Oxidation of hexacyanoferrate(II)

In first experiments, the RAM electrode was held at a fixed potential of +0.6 V vs. SCE, corresponding to mass-transport limited oxidation of hexacyanoferrate(II). Fig. 1 shows current transients obtained for the three dispension rates. Comparison with data for macroelectrodes [8,9] shows a much slower rise to

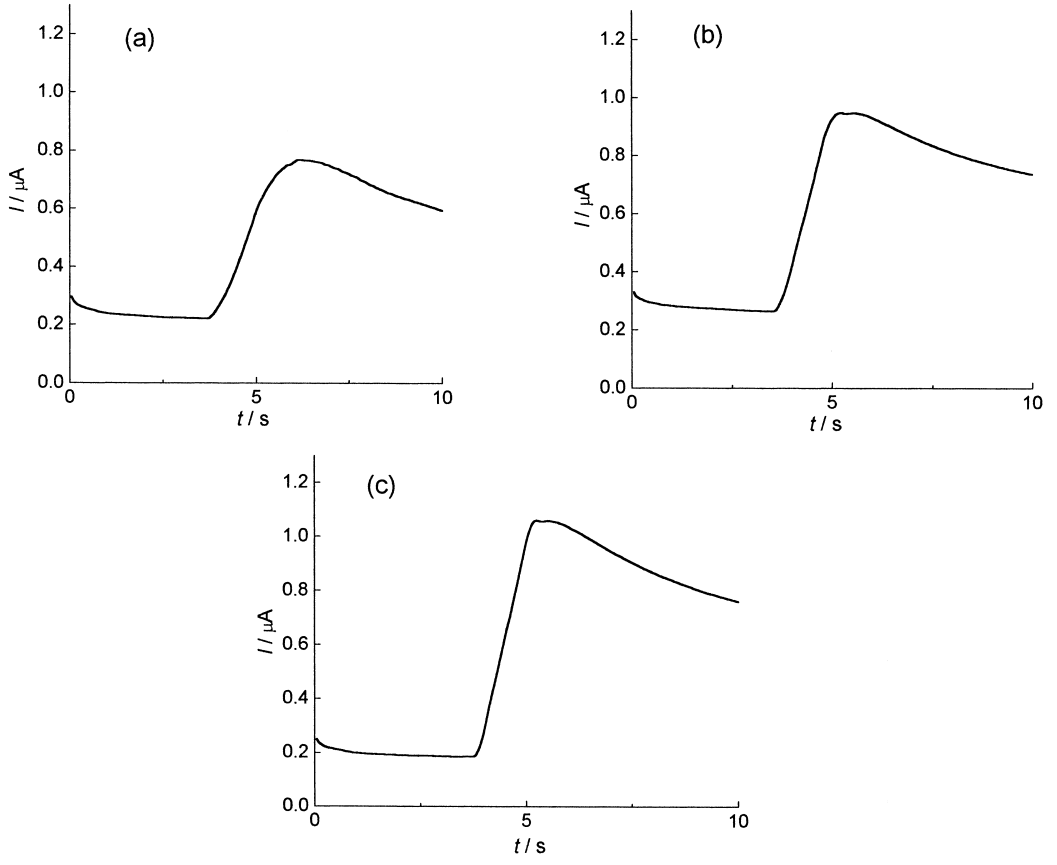

Fig. 1. Oxidation of 2.0 mM $K_4Fe(CN)_6$ in 0.4 M K_2SO_4 electrolyte at RAM electrode. BIA transients recorded at +0.6 V vs. SCE at flow rates: (a) 24.5; (b) 47.6 and (c) 75.3 μl s^{-1}.

the maximum current values and a much slower decrease after the end of the injection period. Indeed, in the case of the lowest flow rate, a plateau is only just reached before the end of the injection. Plotting these maximum currents against flow rate to the power of 3/4 gives a straight line, as predicted for wall-jet hydrodynamics [15], and as for the macroelectrode [9], but with a larger positive intercept. Thus there is a flow-rate effect with this electrode array, indicative that at least some of the microdisk electrodes are sufficiently close that their diffusion fields overlap.

Maximum sensitivity in BIA amperometry will be obtained if the maximum current is reached before the end of injection; there is thus a minimum injection volume for this to be achieved. A plot of maximum current vs. injected volume is shown in Fig. 2, which suggests that at least 70 μl should be injected. At a macroelectrode, the equivalent minimum volume was 20 μl [8]; however, note that at the RAM electrode 75% of the maximum current has been reached already at 20 μl. It may also be that the kinetics of the electrode reaction are slower at the carbon fibre electrode, which would also contribute to a slower approach to the maximum value.

Cyclic voltammograms were also recorded; examples are shown in Fig. 3. These demonstrate the steady-state shape expected from a microelectrode array, but also show some apparent scan-rate dependence. The minimum scan rate to ensure that the whole potential scan takes place during injection at the slowest flow rate is 500 mV s^{-1} (Fig. 3(c)). The importance of carrying out the full scan during injec-

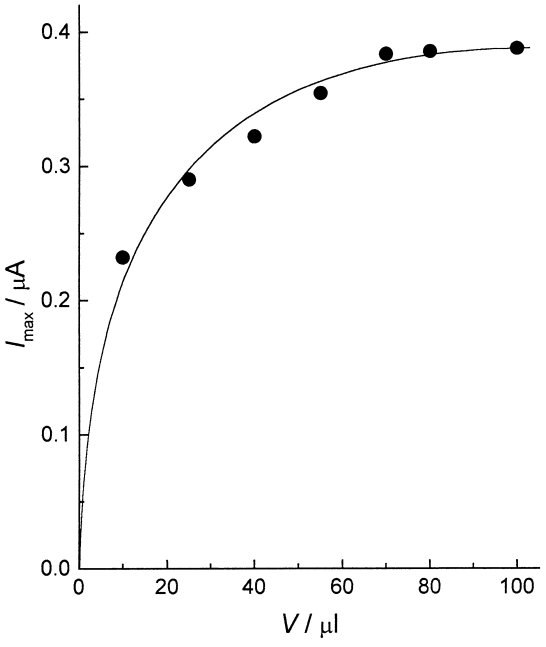

Fig. 2. Plot of maximum current vs. injected volume for BIA of hexacyanoferrate(II) oxidation; flow rate 24.5 μl s^{-1}. Other experimental parameters as in Fig. 1.

tion is less at a RAM electrode than at a macroelectrode (compare 250 and 500 mV s^{-1} scan rates in Fig. 3(b) and (c) which lead to very similar cyclic voltammograms) but Fig. 3(a) (100 mV s^{-1} scan rate) shows substantially lower currents. However, the latter does show the interesting feature that although approximately 80% of the voltammogram is registered after the end of the injection, the currents do not noticeably die away. This ability to suck in electroactive species from a large zone round the electrode in such a fashion has important implications for anodic stripping voltammetry, and will be further discussed below.

Calculation of the individual steady-state current from the equation [1]

$$I = 2nFdDc_{\infty}, \quad (1)$$

where d is the microelectrode diameter (7.0 μm), D the diffusion coefficient of the electroactive species (6.2×10^{-6} cm^2 s^{-1} [16]), c_{∞} the concentration of electroactive species (2.0×10^{-6} mol cm^{-3}), n the number of electrons transferred and F is the Faraday constant, gives a value of 1.68 nA per independent microelectrode. The total currents at low convection rates reach ~1.0 μA, which suggests that there are approximately 600 active microdisks.

The hysteresis in Fig. 3 between forward and reverse scans is observed at all scan rates, increasing linearly with scan rate; from this we can estimate a constant capacitive current over this potential range 0.2 μA, corresponding to 20 μF cm^{-2}.

3.2. Anodic stripping voltammetry

The carbon fibres of the RAM electrode were covered with mercury to make a mercury RAM (MRAM) electrode following the procedure indicated previously [10,11] and described in Section 2. It is clear that at a RAM electrode the surface will be covered by an array of mercury droplets. Nevertheless, even at large glassy carbon electrodes, it was shown [17], that the film is a collection of closely spaced mercury droplets – the close spacing means that the diffusion field completely overlaps and it is described as a mercury thin-film electrode (MTFE).

Important parameters were evaluated from the square wave ASV (SWASV) of Pb^{2+}, see Fig. 4. This shows the dependence on deposition time of the stripping peak current. Owing to the high concentration gradients, after the end of the sample injection the deposition current does not decrease to zero as occurs at a macroelectrode except over very long time period. This is another manifestation of the microelectrode effect discussed above in relation to the cyclic voltammetry of hexacyanoferrate(II) and the fact that the absolute analyte consumption is less, so that the time period necessary to consume the species in the vicinity of the RAM electrode is longer. Such a result has important implications: it demonstrates that there will be a significant memory effect unless blank solution is injected over the MRAM electrode between successive sample injections in order to completely clean the zone of the electrode from any vestiges of Pb^{2+} remaining in the zone of the electrode ensemble.

The microelectrode effect also has implications concerning injected volume and injection flow rate, Fig. 5. In the former case, Fig. 5(a), an injected volume of 70 μl leads to the maximum peak current (>97% of this value for 50 μl injection). This means, as suggested earlier for a macroelectrode [11], that it is useful to inject 25 μl four times: there is a 10% loss of

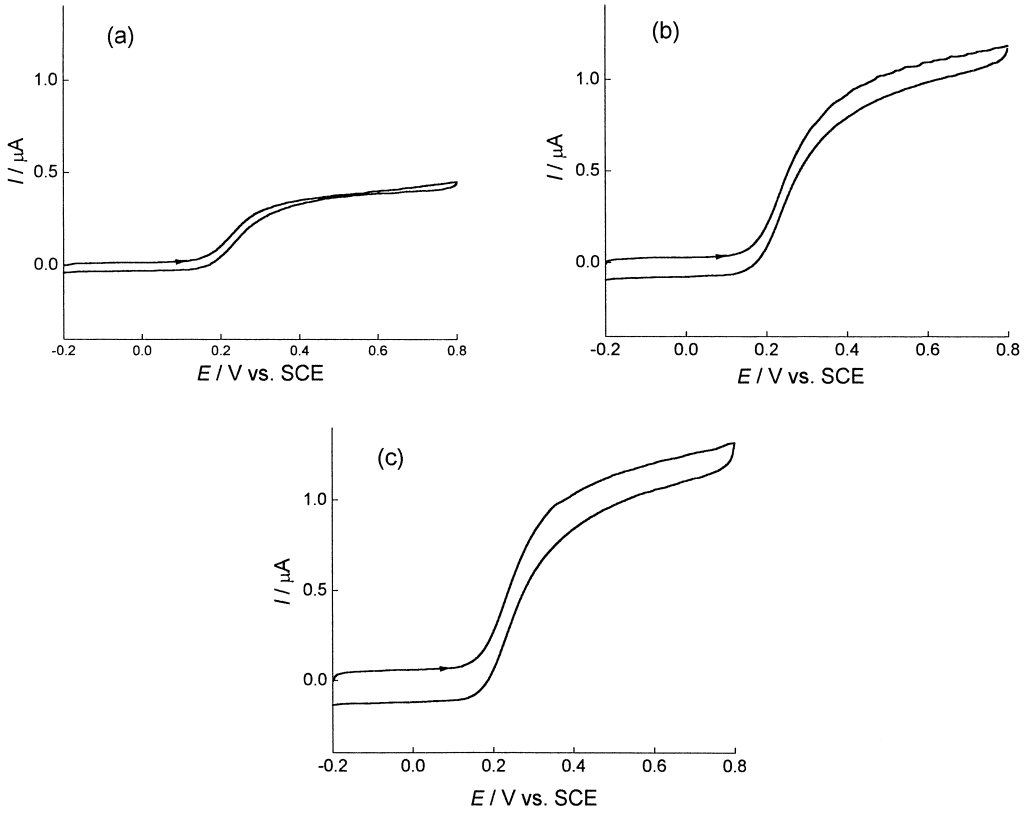

Fig. 3. Cyclic voltammograms for oxidation of 2.0 mM $K_4Fe(CN)_6$ in 0.4 M K_2SO_4 at RAM electrode, 100 μl injection at flow rate 24.5 μl s^{-1}. Scan rate: (a) 100; (b) 250 and (c) 500 mV s^{-1}.

signal compared to 100 μl for individual injections, so that four consecutive injections of 25 μl lead to a total amplification factor of 3.6 with respect to a single 100 μl injection (at a macroelectrode the sensitivity enhancement is 2.5 [11]). Injection flow rate dependence is less than in the equivalent experiment at a macroelectrode [10]: the slowest and middle flow rates give essentially the same stripping current response, so that either can be employed. The predicted $V_f^{-1/4}$ dependence of electrolysis efficiency on injection rate from wall-jet hydrodynamics [15] is not followed due to the continuing accumulation of species after the end of injection – this tends to annul the differences between the different flow rates. This was found at macroelectrodes [10] and is even more evident at RAM electrodes due to the stronger diffusion field.

A BIA–SWASV voltammogram for a mixture of metal ions is shown in Fig. 6. As can be seen, definition of signals is best for Pb and Cd; for Zn the signal is less easy to distinguish from the background. Although it is always found that the signals for lead are larger than the signals for cadmium at MTFEs, which can be attributed to kinetic effects, this difference is accentuated at the MRAM electrodes.

Some calibration data obtained from BIA–SWASV experiments are collected in the second row of Table 1, and can be compared with similar data obtained at an MTFE, first row. Detection limits (3σ) are 5.4 nM for lead and 2.8 nM for cadmium for single injections of 100 μl, which decreases to 1.5 nM and 0.8 nM, respectively, if four consecutive injections of 25 μl are done. The sensitivity enhancement of the MRAM relative to the MTFE (macroelectrode, diameter 0.5 cm) can be calculated as approximately 75 for lead and 7 for cadmium.

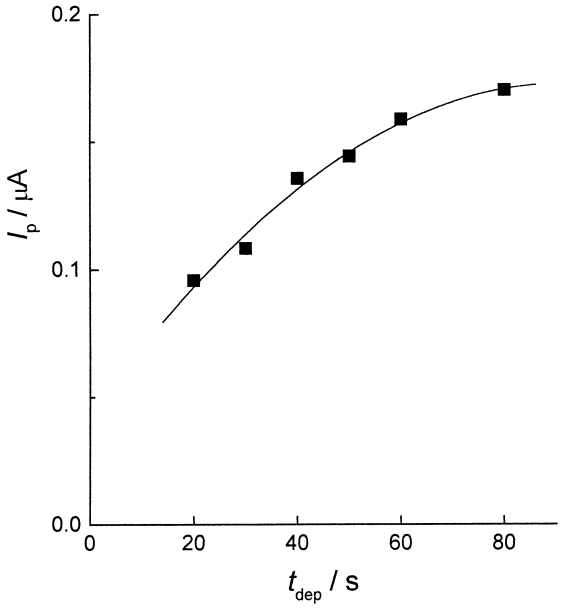

Fig. 4. BIA–SWASV of 10^{-7} M Pb^{2+} in 0.10 M KNO_3+5 mM HNO_3 electrolyte at MRAM electrode, E_{dep}= −1.0 V vs. SCE, 50 μl injection, injection flow rate 24.5 μl s^{-1}. Square-wave parameters: frequency 100 Hz, amplitude 25 mV, scan increment 2 mV. Dependence of stripping peak current, I_p, on preconcentration time, t_{dep}.

Table 1
Linear regression of calibration data for lead and cadmium determinations by BIA–SWASV using MTFE, MRAM and NCMRAM electrodes (for details see text)

Electrode	Slope (nA nM^{-1})	Intercept (μA)	Regression coefficient
MTFE			
Pb	41.0	0.43	0.995 (n=5)
Cd	30.0	0.50	0.995 (n=5)
MRAM			
Pb	1.84	0.09	0.995 (n=5)
Cd	0.12	0.40×10^{-3}	0.998 (n=5)
NCMRAM			
Pb	0.91	6.20×10^{-3}	0.999 (n=5)
Cd	0.12	0.06	0.995 (n=6)

3.3. Anodic stripping voltammetry at a Nafion-coated electrode

Further experiments were carried out at a Nafion-coated MRAM (NCMRAM) electrode assembly, prepared according to the procedure described in Section 2. The purpose of the Nafion film is twofold. First, it helps to fix the mercury droplets in position mechanically and does not allow them to migrate over the RAM electrode surface; this was verified in that after more than 10 injections without the Nafion coating and mercury film renewal, the stripping signal began to decrease whereas with the Nafion coating this did not occur even after many tens of injections.

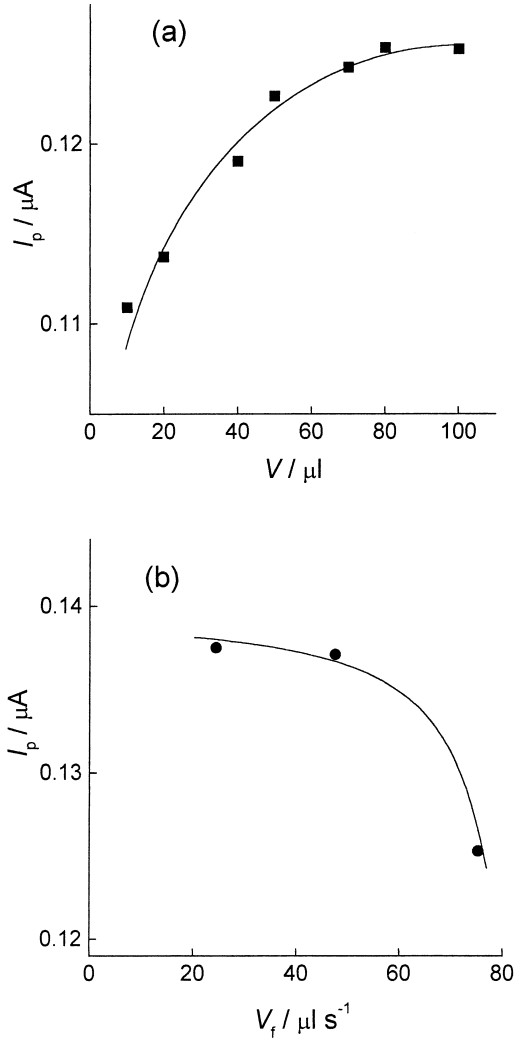

Fig. 5. BIA–SWASV of 10^{-7} M Pb^{2+} in 0.10 M KNO_3+5 mM HNO_3 at MRAM electrode; E_{dep}=−1.0 V vs. SCE, t_{dep}=30 s. Square-wave parameters as in Fig. 4. Effect on stripping peak current, I_p, of: (a) injection volume–flow rate 24.5 μl s^{-1}; (b) flow rate–injection volume 50 μl.

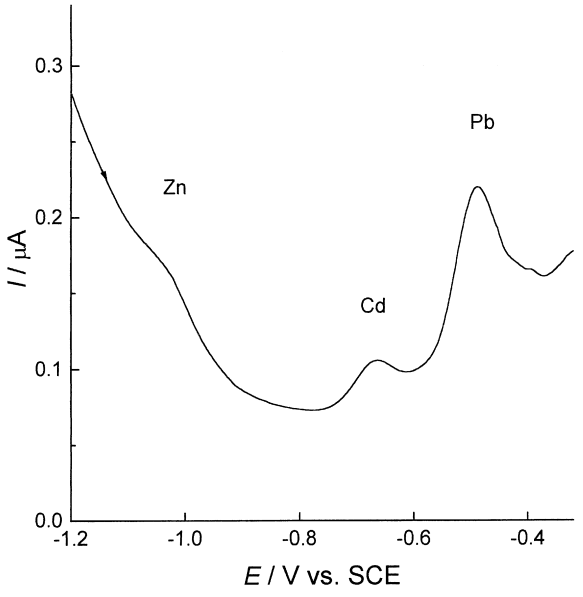

Fig. 6. BIA–SWASV of 10^{-7} M Zn^{2+}, Cd^{2+} and Pb^{2+} in 0.10 M KNO_3+5 mM HNO_3 at MRAM electrode; E_{dep}=−1.4 V vs. SCE, t_{dep}=30 s, injection flow rate 24.5 μl s^{-1}, injection volume 50 μl. Square-wave parameters as in Fig. 4.

Secondly, it reduces contamination from unwanted (mainly organic) interferents in real samples [11].

The dependencies on injection volume and flow rate (analogous to Fig. 5) are shown in Fig. 7 and are essentially the same. Currents are lower, particularly for lead, a reflection of diffusion limitations through the Nafion film. However, Fig. 8 demonstrates that better resolution between components in mixtures is obtained. Once again, calibration data are collected in Table 1.

With Nafion coatings the lead sensitivity drops with respect to the uncoated MRAM electrode due to diffusion limitations; in the case of cadmium the kinetic limitation is such that there is no effect from diffusion limitation. Detection limits (3σ) were calculated as 3.6 nM and 4.7 nM for Pb and Cd, respectively, for single injections, corresponding to 1.0 and 1.3 nM for four successive injections of 25 μl. Compared with the macroelectrode equivalent (4.0 and 2.0 nM, respectively [11]), detection limits are lower by a factor of at least 1.5 at MRAM electrodes. Sensitivity as a function of normalised electrode area can be estimated as 38 and 7 times larger for lead and cadmium, respectively.

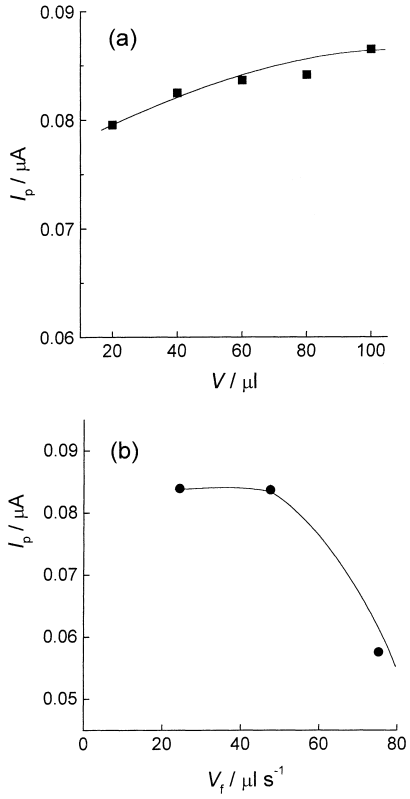

Fig. 7. BIA–SWASV of 10^{-7} M Pb^{2+} in 0.10 M KNO_3+5 mM HNO_3 at NCMRAM electrode; E_{dep}=−1.0 V vs. SCE, t_{dep}=30 s. Square-wave parameters as in Fig. 4. Effect on stripping peak current, I_p, of: (a) injection volume–flow rate 24.5 μl s^{-1}; (b) flow rate–injection volume 50 μl.

Thus NCMRAM electrodes offer an alternative strategy for BIA with modestly improved detection limits, and may be of particular interest in extreme situations where the advantages conferred by the use of microelectrodes are necessary.

4. Conclusions

It has been demonstrated that random arrays of microelectrodes reduce detection limits and improve sensitivity in electrochemical BIA with anodic stripping voltammetry. Although BIA–ASV can be performed directly on real samples without added electrolyte, the combination with microelectrodes, which by themselves permit measurements in highly resistive media and higher electrolysis efficiencies, may prove to be very valuable in extreme situations.

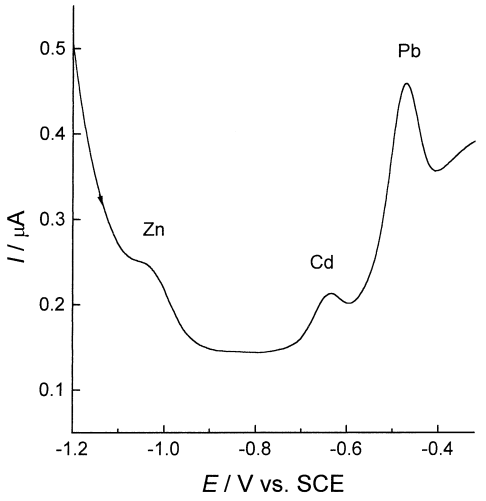

Fig. 8. BIA–SWASV of 10^{-7} M Zn^{2+}, Cd^{2+} and Pb^{2+} in 0.10 M KNO_3+5 mM HNO_3 at NCMRAM electrode; E_{dep}=−1.4 V vs. SCE, t_{dep}=30 s, injection flow rate 24.5 μl s^{-1}, injection volume 50 μl. Square-wave parameters as in Fig. 4.

Acknowledgements

D.A. Fungaro thanks FAPESP, Brazil, for a post-doctoral fellowship. The support of Fundação para a Ciência e Tecnologia, project PEAM/SEL/526/95, is gratefully acknowledged. We thank Dr. S. Fletcher, CSIRO, Melbourne, Australia, for the gift of a RAM electrode.

References

[1] M.I. Montenegro, M.A. Queirós, J.L. Daschbach (Eds.), Microelectrodes: Theory and Applications, Kluwer, Dordrecht, 1991.
[2] R.J. Forster, Chem. Soc. Rev. 23 (1994) 289.
[3] A.M. Bond, Analyst 119 (1994) R1.
[4] B.R. Scharifker, J. Electroanal. Chem. 240 (1988) 61.
[5] S.G. Weber, Anal. Chem. 61 (1989) 295.
[6] H.P. Nirmaier, G. Henze, Electroanalysis 9 (1997) 619.
[7] J. Wang, Z. Taha, Anal. Chem. 63 (1991) 1053.
[8] C.M.A. Brett, A.M. Oliveira Brett, L.C. Mitoseriu, Electroanalysis 7 (1995) 225.
[9] C.M.A. Brett, A.M. Oliveira Brett, L.C. Mitoseriu, Anal. Chem. 66 (1994) 3145.
[10] C.M.A. Brett, A.M. Oliveira Brett, L. Tugulea, Anal. Chim. Acta 322 (1996) 151.
[11] C.M.A. Brett, A.M. Oliveira Brett, F.-M. Matysik, S. Matysik, S. Kumbhat, Talanta 43 (1996) 2015.
[12] C.M.A. Brett, A.M. Oliveira Brett, L. Tugulea, Electroanalysis 8 (1996) 639.
[13] S. Fletcher, M.D. Horne, RAM™ Electrodes – An Introduction, CSIRO Division of Minerals, Port Melbourne, Australia, 1995.
[14] M.E.R. Dam, K.N. Thomson, P.G. Pickup, K.H. Schroder, Electroanalysis 7 (1995) 70.
[15] C.M.A. Brett, A.M. Oliveira Brett, Electrochemistry. Principles, Methods and Applications, Oxford University Press, Oxford, 1993, pp. 155–157.
[16] C.M.A. Brett, A.M. Oliveira Brett, A.C. Fisher, R.G. Compton, J. Electroanal. Chem. 334 (1992) 57.
[17] F.-M. Matysik, S. Matysik, A.M. Oliveira Brett, C.M.A. Brett, Anal. Chem. 69 (1997) 1651.